

FIRST FULL EVOLUTIONARY COMPUTATION OF THE HE-FLASH INDUCED MIXING IN POPULATION II STARS.

SANTI CASSISI^{1,3}, HELMUT SCHLATTI^{2,3}, MAURIZIO SALARIS^{2,3} AND ACHIM WEISS³

Draft version August 6, 2018

ABSTRACT

The core helium-flash in low-mass stars with extreme mass loss occurs after the tip of the RGB, when the H-rich envelope is very thin. The low efficiency of the H-shell source enables the He-flash driven convective zone to penetrate H-rich layers and trigger a thermonuclear runaway, resulting in a subsequent surface enrichment with He and C. In this work we present the first full computations of Population II low-mass stellar models through this phase. Models experiencing this dredge-up event are significantly hotter than their counterparts with H-rich envelopes, which makes them promising candidates for explaining the existence of stars observed beyond the canonical blue end of the horizontal branch (“blue hook stars”). Moreover, this temperature difference could explain the observed gap in M_V between extreme blue horizontal-branch and blue hook stars. A first comparison with spectroscopic observations of blue hook stars in the globular cluster ω Cen is also presented.

Subject headings: stars: abundances — stars: evolution — stars: horizontal branch — stars: late-type

1. INTRODUCTION

The Horizontal Branch (HB) in the Color-Magnitude Diagram (CMD) of a number of Galactic Globular Clusters (GGCs), like e.g. NGC 6752, shows extended blue tails populated by so called Extreme HB (EHB) stars, characterized by extremely high effective temperatures. The existence of these EHB stars is hard to interpret in terms of canonical stellar evolution, where the He-flash takes place at the tip of the Red Giant Branch (RGB)⁴. None of those stars would have a hot enough HB locus to explain the extended blue tail of, e.g., NGC 6752 (see, e.g., Moehler et al. 2000). Castellani & Castellani (1993) have suggested the so-called “delayed helium-flash” (“delayed HEF”) scenario to explain the existence of EHB stars. This scenario envisages that, as a consequence of an high mass-loss efficiency during the Red Giant Branch (RGB) evolution (due to enhanced stellar wind and/or dynamical interactions with other stars in the dense cluster core), a star can lose so much envelope mass that it fails to ignite the HEF at the tip of the RGB, thus evolving toward the White Dwarf (WD) cooling sequence with an electron-degenerate helium core. Depending on the amount of the residual H-rich envelope mass, the star will still ignite He-burning either at the bright end of the WD cooling sequence (“early” hot flasher, hereafter EHF), or along the WD cooling sequence (“late” hot flasher, hereafter LHF). After the He-flash these stars will settle on the Zero Age HB (ZAHB) and with their strongly reduced envelope mass they are much hotter than their counterparts on the canonical ZAHB.

Recent far-UV photometric observations of the GGC ω Cen (see e.g. D’Cruz et al. 2002) and NGC2808 (Brown et al. 2001, B01) have disclosed the existence of a spread in the UV brightness at the hot end of the observed HB stars, larger than the expected photometric errors, and

with a sizable number of stars appearing to form a hook-like feature. These “blue hook” stars are located even beyond the hot end of EHB objects like the ones observed in NGC 6752 (Moehler et al. 2002, M02), and are fainter than the bluest end of the canonical ZAHB locus by up to about 0.7 mag in the UV. The evolution of EHF and their possible connection with blue hook stars have been investigated by D’Cruz et al. (2000), but the progeny of such EHF is not hot enough to explain the existence of “blue hook” stars.

A more promising working scenario has been suggested by Sweigart (1997, S97) based on the evolution of LHF. He finds that the convection zone produced by the late HEF is able to penetrate into the H-rich envelope, thereby mixing H into the hot He-burning interior (He-flash mixing, hereafter HEFM) where it is burned rapidly. A consequent dredge-up of matter which has been processed via both H- and He-burning enriches the outer envelope by He and some carbon and nitrogen. According to S97 these abundance changes cause a discontinuous increase of the HB effective temperature at the transition between un-mixed and mixed models, producing a gap at the hot end of the HB stellar distribution as indeed observed by Bedin et al. (2000) in NGC2808. At the same time the changes of the surface chemical composition induced by the HEFM modify the emergent spectral energy distribution, and may explain the fact that these stars appear as subluminous objects in the UV CMD.

This scenario has been examined in more detail by B01, but their computations were stopped at the onset of the HEFM, due to the numerical difficulty of following the development of this process and the simultaneous nucleosynthesis within the convection zone. B01 could therefore only estimate the surface chemical abundances after the

¹INAF - Osservatorio Astronomico di Collurania, Via M. Maggini, I-64100 Teramo, Italy; cassisi@te.astro.it

²Astrophysics Research Institute, Liverpool John Moores University, Twelve Quays House, Egerton Wharf, Birkenhead CH41 1LD, UK; hs.ms@astro.livjm.ac.uk

³Max-Planck-Institut für Astrophysik, Karl-Schwarzschild-Strasse 1, D-85748 Garching, Germany; aweiß@mpa-garching.mpg.de

⁴In this sense we understand the canonical HB to consist of stars igniting He at the tip of the RGB.

HEFM episode, and the resulting ZAHB effective temperature. In this paper we present the first full computation of LHF star evolution, following the development and outcome of the HEF and HEFM; in this way we are able to consistently predict the effect of the HEFM process on the chemical stratification of the stellar envelope, thus eliminating the need to assume an ad-hoc chemical distribution for the post-HEFM phase.

In §2 we briefly introduce our computational code and present the evolutionary sequences for LHF stars. The resulting model properties are compared with the models and estimates of B01. In the final section our results are briefly compared with relevant observations.

2. EVOLUTION OF LHF STARS

A consistent calculation of the HEFM process is challenging, because the timescale for proton-capture reactions within the flash-convection zone is comparable to the convective mixing timescale; therefore the latter has to be treated time-dependently and solved simultaneously with the nuclear network. Due to the evident numerical difficulties in the only available computation of a low-mass star experiencing HEFM performed by S97, the energy contribution provided by the H-burning was not accounted for. This is clearly a too crude approximation since it causes an underestimate of the extent of the mixed region and, thus, of the final effects on the chemical composition of the outer layers.

In order to perform the first full evolutionary calculations of stars undergoing HEFM, we adopt an evolutionary code (Schlattl et al. 2001, 2002, hereafter S01, S02) in which the equations for convective mixing and nuclear burning are solved in one common scheme, and which accounts for the simultaneous burning of both H and He. The time-dependent mixing is treated as a fast diffusive process, where the diffusion coefficient is proportional to the convective velocity derived from a convection theory (S01). The reliability and accuracy of this approach has been already discussed by S01 and S02, in their investigation of HEFM in extremely metal-poor stars during the core He-flash at the tip of the RGB.

We have computed several sequences of evolutionary models starting from the same $0.862 M_{\odot}$ progenitor, with initial metallicity $Z = 0.0015$ and helium abundance $Y = 0.23$. This choice is the same made by B01, and provides an age for the models at the RGB tip of about 12.6 Gyr, in agreement with current estimates of GGC ages (e.g., Salaris & Weiss 2002). The sequences are characterized by different amount of mass loss along the RGB, parameterized according to the standard Reimers (1975) relation; we will denote the different sequences according to the value adopted for the free mass-loss parameter η . We have considered values of η in the range between 0.0 and 0.65, in order to have models igniting the HEF at the RGB tip, as EHF stars or as LHF stars.

Figure 1 shows the evolution in the H-R diagram of models computed with different values of η , which experience the HEF in different evolutionary phases. We have found that the largest η leading to the HEF at the RGB tip is 0.55, whereas a value of about 0.58 provides a mass-loss efficiency corresponding to EHF stars. These two se-

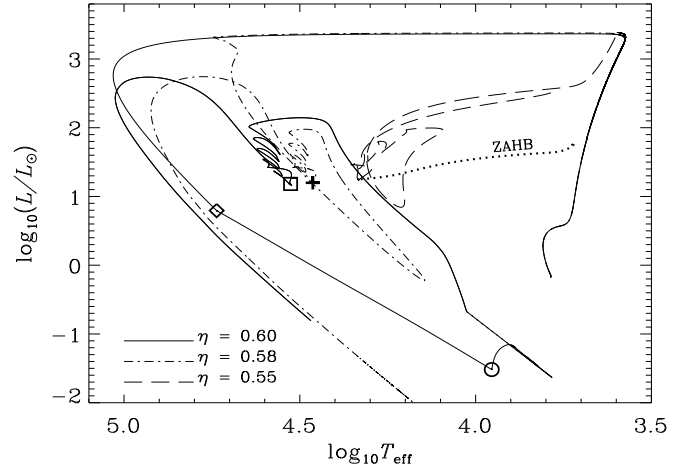


FIG. 1.— The H-R diagram of some evolutionary models computed accounting for different values (as labeled) of the Reimers mass-loss parameter. The canonical ZAHB is also shown (dotted line) together with the evolution along the Main Sequence and RGB of the progenitor. The ZAHB location of the sequence with $\eta = 0.58$ is marked by '+', while the onset of the HEF, the H-mixing event, and the consequent ZAHB location of the $\eta = 0.60$ sequence are denoted by ' \diamond ', ' \circ ', and ' \square ', respectively.

quences have the same He-core mass ($0.4930 M_{\odot}$) at the HEF but very different envelope masses of $0.0192 M_{\odot}$ and $0.0012 M_{\odot}$, respectively, which leads to a difference of ~ 7500 K in the ZAHB effective temperature of these models (i.e. ~ 21500 K against ~ 29000 K, respectively). These two models do not experience HEFM — thus maintain H-rich envelopes — and share the same structural properties during the major HEF as expected on the basis of the results obtained by Castellani & Castellani (1993) and B01.

The situation changes drastically when a slightly higher value of η is used. The sequence computed with $\eta = 0.60$ ignites the HEF along the WD cooling sequence; in this case the events following the core HEF are completely different from the evolution of models computed with a lower η . The HEF ignition is located $0.141 M_{\odot}$ off center⁵, when $\log(L/L_{\odot}) = 0.79$; in this phase the luminosity produced by the H-burning shell is $\sim 0.35 L_{\odot}$ and the He-core mass is equal to $0.4907 M_{\odot}$, i.e., $0.0023 M_{\odot}$ lower than in the model computed with $\eta = 0.58$. The envelope mass is equal to $5.5 \times 10^{-4} M_{\odot}$, about half the value of the model with $\eta = 0.58$.

Soon after the HEF ignition the surface luminosity drops and the peak of the flash luminosity ($L_{\text{He}} = 3.7 \times 10^{10} L_{\odot}$) occurs when the surface luminosity is equal to $\log(L/L_{\odot}) = 0.36$, about 1000 years after the onset of the HEF. The expansion of the core during the flash episode cools down the surrounding layers, and when the HEF is at its peak the energy contribution provided by the H-burning shell drops to $L_{\text{H}} \approx 4.9 \times 10^{-3} L_{\odot}$. Due to the huge energy flux caused by the HEF a convective region develops above the point where He ignites. This convection zone reaches the H-rich envelope and mixes protons from the envelope into the hot He-burning interior when the stellar luminosity is equal to $\log(L/L_{\odot}) = -1.2$ and the energy provided by H- and He-burning are $2.7 \times 10^{-6} L_{\odot}$ and $1.1 \times 10^{-7} L_{\odot}$, respectively. This HEFM

⁵We consider the HEF to start when the He-burning luminosity is equal to $100 L_{\odot}$, as in Sweigart & Gross (1978).

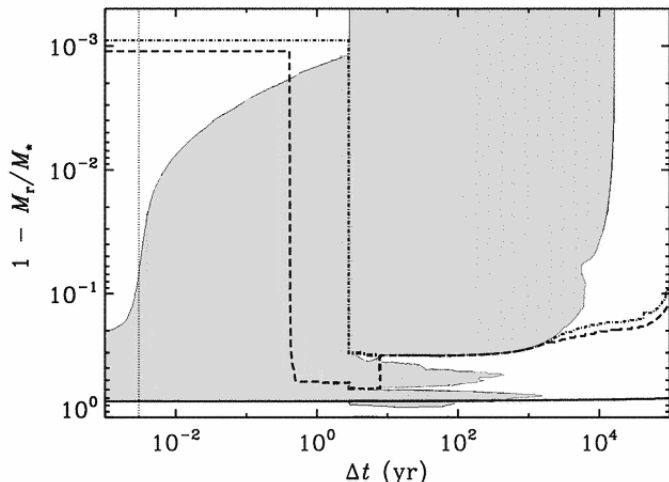


FIG. 2.— Evolution from the beginning of the HEF of the different convective zones, indicated by shaded areas, in our model with $\eta = 0.60$. The solid, dashed, and dot-dashed line denote the mass location of maximum energy release by He-burning, CNO cycle, and p - p chain, respectively. The vertical dotted line marks the moment of the HEF peak luminosity; the zero point in time has been chosen to be one day before this moment.

event occurs about 5 months after the HEF was at maximum.

The evolution and the main properties of this LHF model up to this point are in good agreement with the results obtained by B01 for the corresponding model with the smallest mass-loss efficiency necessary to undergo HEFM. B01's values for the He-core mass and envelope mass are $0.491 M_\odot$ and $6.0 \times 10^{-4} M_\odot$, respectively, very similar to our results. However, the minimum η necessary to have a LHF with HEFM is equal to 0.818 in B01 models, while we need a much lower value of 0.60, which means that our models lose more mass than the ones of B01. Our models are on average cooler than theirs during the HB phase (e.g., the ZAHB effective temperature of our hottest model not experiencing HEFM is lower than in B01) and therefore they are possibly also cooler along the RGB where large part of the mass loss happens. Since, according to the Reimers relation cooler models tend to lose more mass at a fixed value of η , this would explain the smaller value of η needed in our models. The fact that our hottest model without HEFM is cooler by about 1500 K than the one in B01, cannot be explained by our coarser η resolution, as, e.g., models with $\eta = 0.58$ and 0.59 differ only by about 500 K in their ZAHB location (Table 1).

Whereas B01 stopped their computation at the beginning of the H ingestion by the He-flash driven convection zone, we are able to follow consistently the evolution through this event, and thus obtain reliable estimates of the variation of the relevant surface chemical abundances. This is important not only in order to predict the spectral energy distribution of these stars, but also to provide quantitative estimates for comparison with spectroscopic observations of "blue hook" stars.

The evolution of the convective zones in the $\eta = 0.60$ sequence after the onset of the HEF, as well as the location of the layers where the H- and He-burning energy release are at maximum, are shown in Figure 2. As soon as H is carried into the interior, it starts burning through the CNO cycle at an extremely large rate, because of the high

temperatures in these layers and the large abundance of ^{12}C nuclei produced by the 3α reactions; at the same time the upper boundary of the flash-induced convective region moves further outward, eventually reaching the stellar surface. The maximum energy released by H burning is equal to $8.2 \times 10^9 L_\odot$; the stellar luminosity then is equal to $\log(L/L_\odot) = -1.37$.

The main consequence of the strong H-burning is that the flash-induced convective zone splits initially into two and then even into three separate convective regions because of temporarily three active burning shells, i.e., the He-burning shell and two shells related to H-burning through the p - p chain and the CNO cycle, respectively (Fig. 2). We note that this process is similar to the one occurring in low-mass, extremely metal-poor stars at the RGB tip, see S01 and also B01. Because of the extremely thin envelope mass, the star does not expand to a RGB configuration, despite the large additional amount of energy injected into the envelope by the H-burning shell. The total amount of H burned during the HEFM episode is about $3.7 \times 10^{-4} M_\odot$ and the final mass fraction of H in the envelope is 4×10^{-4} , which is very low but still non-negligible (see §3). A large amount of matter processed by both H- and He-burning is dredged to the surface, changing its chemical composition. In particular, the final total metallicity Z is equal to 0.0365; the metal distribution is strongly C-enhanced, the carbon mass fraction being equal to 0.029, while the surface abundances of oxygen and nitrogen are 3.5×10^{-5} and 0.007, respectively. In addition, the surface He abundance increases to $Y = 0.96$.

After the envelope H is strongly reduced and the electron degeneracy is lifted in the core region close to the HEF ignition, the three convective shells disappear. Like in standard He-flash models the He-burning shell slowly moves toward the center via a few additional HEFs (no HEFM ensues), removing the electron degeneracy in the whole He-core. Finally, the star settles on its ZAHB location at $\log(L/L_\odot) = 1.18$ and $T_{\text{eff}} = 33\,600$ K (see Fig. 1); the corresponding bolometric magnitude is about 0.14 mag higher than for the hottest canonical ZAHB model, due to the slightly smaller He-core mass at the HEF. (A summary of the ZAHB locations of the models with different mass-loss parameter η is provided in Table 1.)

The HB progeny of the $\eta = 0.59$ model, i.e., the least massive one which does not experience the HEFM process, shows a ZAHB effective temperature equal to about 30 000 K (close to "+" in Fig. 1). The discontinuity of the ZAHB effective temperature between models with and without HEFM is therefore $\sim 3\,600$ K. This value is however only a lower limit to the real discontinuity; in fact, although radiative opacities for the correct He and H abundances have been used, the metal distribution was taken to be scaled solar, not C-enriched as would be appropriate for the post HEFM objects. A comparison of OPAL (see,

TABLE 1
ZAHB LOCATION OF SELECTED MODELS

η	0	0.55 ^a	0.58	0.59	0.60
$\log(L/L_\odot)$	1.76	1.24	1.20	1.19	1.18
$\log T_{\text{eff}}$	3.722	4.332	4.463	4.474	4.526

^a Hot end of canonical HB

e.g., Iglesias & Rogers 1996) scaled-solar opacity tables with C-enriched ones for Y and Z values nearly equal to the actual surface composition of our $\eta = 0.60$ model reveals that the radiative opacities have been overestimated by up to 50%.

By crudely applying this correction to the opacity in a post-HEFM model before settling on its ZAHB, we estimate that the ZAHB location of our C-enriched models should be about 1500 K hotter. This increases the T_{eff} -discontinuity between models with and without HEFM to ~ 5100 K. Although B01 could not obtain the final surface chemical composition of their LHF's from full evolutionary computations, their post-HEFM ZAHB models with He-C mixture assume $Y = 0.96$ and a carbon mass fraction of 0.04, both values being very similar to the outcome of our detailed computation. Employing the appropriate opacities B01 determined a discontinuity in the ZAHB T_{eff} distribution of ≈ 6000 K, similar to the value we would obtain in case of using opacities with the correct metal distribution.

3. FINAL REMARKS

In the previous section we have shown that our full computations through the HEFM phase do support the evolutionary scenario for blue hook stars outlined by B01. The most important changes induced by the HEFM process are related to the surface chemical composition, which is modified in a drastic way with respect to the initial pattern due to the mixing of matter processed by both H- and He-burning. In order to compare theory with observations one needs spectroscopic analyses of samples of blue hook stars in GGCs.

Very recently, a spectroscopic analysis of a sample of blue hook stars in ω Cen has been published by M02. On the basis of medium resolution spectra M02 found that the blue hook stars in ω Cen are significantly hotter ($T_{\text{eff}} \geq 35,000$ K) than EHB stars, have on average a solar He-abundance with four objects characterized by $Y \geq 0.7$, and there are indications that their outer layers are C-enhanced, albeit by possibly much less than the value predicted by our models (analogous discrepancy does exist for the S02 computations of the HEFM in extremely metal-poor stars). These results provide some support for the HEFM scenario as a plausible explanation for the existence of blue hook stars. Another important result obtained by M02 is the clear evidence that blue hook stars in ω Cen retain a substantial fraction of their initial H abundance, which is barely reproduced by our models. For instance, in the $\eta = 0.60$ model we obtain $\log(n_{\text{He}}/n_{\text{H}}) \approx 2.8$ whereas the larger value measured by M02 is of the order

of $+0.94 \pm 0.14$, all other values being negative.

A possible cause of this discrepancy is the outward diffusion of H and the gravitational settling of He in the atmospheres of blue hook stars, as already suggested by M02, a process which is not included in our computations. One has also to bear in mind that the residual amount of H left at the surface after the HEFM process is strongly dependent on the mixing efficiency adopted in the evolutionary computations. A smaller efficiency would cause H to be burned at a smaller depth within the star, which would result in a thinner convective region above the H-burning shell, and thus a reduced H-dilution when this zone reaches the surface. Moreover, with the temperature being lower, H would be consumed at a smaller rate. Even if we have not performed a detailed investigation of the effect of a reduced mixing efficiency on our models, we can use our computations of the evolution of extremely metal-poor low-mass stars during the HEF (see S02) to predict that a reduction of the mixing efficiency by a factor 2×10^4 should increase the residual amount of H by an order of magnitude. This would be in better agreement with the smaller value of the ratio $\log(n_{\text{He}}/n_{\text{H}})$ measured in one blue hook star by M02, but still too large to explain the higher H-abundances observed in all other blue hook stars of the M02 sample. It is also worth mentioning that the observed T_{eff} values are generally higher than the values attained by our LHF models.

Before a definitive assessment of the adequacy of the HEFM scenario in explaining the HB blue hook stars is possible, a large observational and theoretical effort is necessary; in particular, one needs to obtain higher quality spectra for a larger sample of GGC blue hook stars to investigate in more detail the evolutionary consequences of the HEFM process on a larger set of models and to study the dependence of the HEFM surface chemical composition changes on the numerical and physical assumptions, on which the computation of the evolution through this phase are based. This last topic will be addressed in a forthcoming paper.

S.C. has been supported by MURST (Cofin2002), and H.S. by a Marie Curie Fellowship of the European Community program "Human Potential" under contract number HPMF-CT-2000-00951. S.C., M.S., and H.S. acknowledge the hospitality of the Max-Planck-Institut für Astrophysik, where part of this work has been carried out. A.W. thanks the Institute for Nuclear Theory at the University of Washington for its hospitality and the Department of Energy for partial support during completion of this work. We are grateful to A.V. Sweigart for constructive discussions.

REFERENCES

Bedin, L.R., Piotto, G., Zoccali, M., Stetson, P.B., Saviane, I., Cassisi, S. & Bono, G. 2000, A&A, 363, 159

Brown, T.M., Sweigart, A.V., Lanz, A.V., Landsman, W.B. & Hubeny, I. 2001, ApJ, 562, 368 (B01)

Castellani, M. & Castellani, V. 1993, ApJ, 407, 649

D'Cruz, N.L., O'Connell, R.W., Rood, R.T., et al. 2000, ApJ, 530, 352

Iglesias, C.A. & Rogers, F.J. 1996, ApJ, 464, 943

Moehler, S., Sweigart, A.V., Landsman, W.B. & Heber, U. 2000, A&A, 360, 120

Moehler, S., Sweigart, A.V., Landsman, W.B. & Dreizler, S. 2002, A&A, 395, 97 (M02)

Reimers, D. 1975, Mem. Royal. Soc. Liege, 8, 369

Salaris, M. & Weiss, A. 2002, A&A, 388, 492

Schlattl, H., Cassisi, S., Salaris, M. & Weiss, A. 2001, ApJ, 559, 1082 (S01)

Schlattl, H., Salaris, M., Cassisi, S., & Weiss, A. 2002, A&A, 395, 77 (S02)

Sweigart, A.V. 1997, in The Third Conference on Faint Blue Stars, ed. A.G. Davis Philip, J. Liebert & R.A. Saffer (Schenectady: L. Davis Press), 3 (S97)

Sweigart, A.V. & Gross, P.G. 1978, ApJS, 36, 405